49th AIAA Aerospace Sciences Meeting including the New Horizons Forum and Aerospace Exposition
4 - 7 January 2011, Orlando, Florida

AIAA 2011-1306

Part 1: The Wind Tunnel Model Design and Fabrication of Cal Poly's AMELIA 10 Foot Span Hybrid Wing-Body Low Noise CESTOL Aircraft

Kristina K. Jameson[1], David D. Marshall[2], Rory Golden[3], and Eric Paciano[4]
California Polytechnic State University, San Luis Obispo, CA, 93407

Robert J. Englar[5] and Richard J. Gaeta[6]
Georgia Tech Research Institute, Atlanta, GA 30332-0844

and

Jay Paterson[7] and Dave Mason[8]
Patersonlabs, Inc., Kent, WA 98031

A collaboration between California Polytechnic Corporation with Georgia Tech Research Institute (GTRI) and DHC Engineering worked on a NASA NRA to develop predictive capabilities for the design and performance of Cruise Efficient, Short Take-Off and Landing (CESTOL) subsonic aircraft. In addition, a large scale wind tunnel effort to validate these predictive capabilities for this NRA for aerodynamic and acoustic performance during takeoff and landing has been undertaken. The model, Advanced Model for Extreme Lift and Improved Aeroacoustics (AMELIA), was designed as a 100 passenger, N+2 generation, regional, cruise efficient short takeoff and land (CESTOL) airliner with hybrid blended wing-body with circulation control and upper surface blowing. The model design was focused on fuel-savings and noise goals set out by the NASA N+2 definition. The AMELIA has a 10 ft wing span. PatersonLabs was chosen to build AMELIA. The National Full-Scale Aerodynamic Complex (NFAC) 40 ft by 80 ft wind tunnel was chosen to perform the large-scale wind tunnel test in the summer of 2011.

I. Introduction

With the very recent advent of NASA's Environmentally Responsible Aviation Project (ERA)[1], dedicated to designing aircraft that will reduce the impact of aviation on the environment, there is a need for research and development of methodologies to minimize fuel burn, emission, and a reduction in community noise produced by regional airlines. ERA is specifically concentrating in the areas of airframe technology, propulsion technology, and vehicle systems integration all in the time frame for the aircraft to be at a Technology Readiness Level (TRL) of 4-6 by the year of 2020 (deemed N+2). The proceeding project looking into similar issues was led by NASA's Subsonic Fixed Wing Project and focused on conducting research to improve prediction methods and technologies that will

[1] Assistant Professor, Aerospace Engineering, San Luis Obispo, Ca 93407, AIAA Member.
[2] Associate Professor, Aerospace Engineering, San Luis Obispo, Ca 93407, AIAA Member.
[3] Graduate Student, Aerospace Engineering, San Luis Obispo, Ca 93407, AIAA Student Member.
[4] Undergraduate Student, Aerospace Engineering, San Luis Obispo, Ca 93407, AIAA Student Member.
[5] Principal Research Engineer, Georgia Tech Research Institute, Atlanta, GA 30332, AIAA Member.
[6] Research Engineer, Georgia Tech Research Institute, Atlanta, GA 30332, AIAA Member.
[7] President, patersonlabs, inc., Kent, WA 98031, AIAA Member.
[8] Model Designer, patersonlabs, inc., Kent, WA 98031, AIAA Member.

produce lower noise, lower emissions, and higher performing subsonic aircraft for the Next Generation Air Transportation System.

The work provided in this investigation was an NRA funded by Subsonic Fixed Wing Project starting in 2007 with a specific goal of conducting a large scale wind tunnel test along with the development of new and improved predictive codes for the advanced powered-lift concepts. These concepts are incorporated into the wind tunnel model and in conjunction with the verification of these codes by the experimental investigation an experimental data base will be obtained during the wind tunnel test. Powered-lift concepts investigated are Circulation Control (CC) wing in conjunction with over the wing mounted engines to entrain the exhaust to further increase the lift generated by CC technologies alone.

There are a number of papers in the past few years presenting computational studies of CC technologies. Most of them have focus on 2D studies.[2-11] While there are a number of excellent 2D experimental datasets available for such CFD validation[12-15], the same is not true for 3D experimental data[16]. This effort aims to address this short fall by creating a comprehensive and relevant 3D database for current and future 3D simulations. Experimental measurements included in the database will be forces and moments, surface pressure distributions, local skin friction, boundary and shear layer velocity profiles, far-field acoustic data and noise signatures from turbofan propulsion simulators. This paper focuses on designing and developing a model with NASA's N+2 goals for less environmental impact as well as the fabrication of a full span wind tunnel model to be used to create the 3D validation database for numerical simulations. Specifically, the model was designed as a 100 passenger, regional, cruise efficient short takeoff and land (CESTOL) airliner with hybrid blended wing-body with circulation control. The configuration was developed by David Hall and refined by Cal Poly. The wind tunnel model was sized by the NRA and the size of available wind tunnels, which scaled the model to a 10 ft span. The resulting design is the Advanced Model for Extreme Lift and Improved Aeroacoustics (AMELIA) and is the subject of two companion papers. Part 1 of this paper will describe the conceptual designs considered for this project, the selected configuration adapted for a wind tunnel model, the internal configuration of AMELIA, and the experimental measurements chosen in order to satisfy the requirement of obtaining an experimental measurement database. Part 2 of this paper (Preparation for Wind Tunnel Model Testing and Verification of Cal Poly's AMELIA 10 Foot Span Hybrid Wing-Body Low Noise CESTOL Aircraft) for a full description the progress of the large-scale wind tunnel test along with the experimental techniques that will be employed during the test. Please see Refs. 19-24 for more details on the predicted performance of this CESTOL aircraft along with the improvements of the predictive codes.

II. AMELIA Design Considerations

NASA is committed to identifying solutions that meet improvement goals for noise, emissions, and energy usage (fuel burn). They have classified the N+2 design metrics as a 40% reduction in fuel consumption, progress towards -42 dB lower noise levels, a 70% decrease in emissions, and a 50% reduction in field length performance over current generation aircrafts. Theoretically the aircraft should reach a Technology Readiness Level (TRL) of 4-6 by the year 2020. Dave Hall at DHC Engineering submitted conceptual designs of four separate configurations to address the N+2 goals with a down selection by Cal Poly to one favorable configuration.

A. Conceptual Designs Considered

Four CESTOL configurations were developed for consideration for the large-scale wind tunnel test. The first - Configuration 1 — has the most conventional appearance, in that it employs the tube-and-wing layout. This configuration utilizes a high aspect ratio wing along with a cruciform tail. Utilizing over the wing mounted engines upper surface blowing is provided, which when combined with circulation control at the trailing edge, creates the powered lift necessary for short takeoff and landing. The inboard section of the wing was specifically designed to enhance flow turning ability during these flight segments. An isometric view of Configuration 1 is provided in Fig. 1.

Figure 1. Configuration 1 is comprised of a high aspect ratio wing, over the wing engines, circulation control at the trailing edge and a cruciform tail.

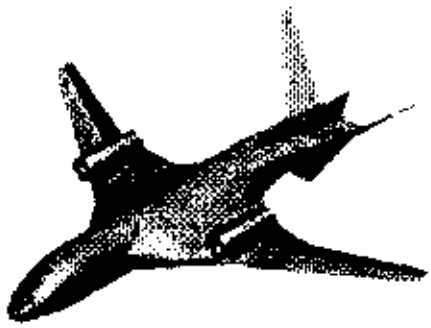

Figure 2. Configuration 2 utilizes a hybrid blended wing body, over the wing mounted engines, a V-tail and circulation control at the leading and trailing edge of the wings.

Drastically different from the first, the second configuration ilizes a Hybrid blended-Wing-Body (HWB). Upper surface owing coupled with leading and trailing edge blowing for rculation control provides powered lift system. The aft fuselage rminates in a beaver tail, where a structural dorsal provides ldition structural support. Configuration 2, shown in Fig 2, nploys a V-tail in conjunction with aft fuselage strakes to aid in ow attachment.

The third configuration was inspired by recent interest in an rcraft utilizing a true Blended-Wing-Body (BWB). This aircraft ncept is a significant departure from the first two aircraft designs that the two turbofan engines are embedded within the very thick ing root; this can be seen in Fig. 3. The exhaust discharges through high aspect ratio 2-D nozzle at the trailing edge of the vehicle. The intent is not only to produce thrust through this nozzle throughout the flight but to create increased flow circulation around the aircraft generating additional lift during takeoff and landing.

The final and most complex design is shown in Fig. 4, termed the Diamond-Wing-Body (DWB). It may be thought of as a Joined-Wing with a vertical structural member joining the fore and aft wings at the outer span points. The intent is to improve local air flow and mitigate shock formation at high subsonic Mach numbers. These vertical members are more like wingtip sails than winglets and act structurally as struts. The forward wing sweeps aft, and the aft wing sweeps forward forming a diamond planform shape in the top view. Both wings have a high aspect ratio. The propulsion system is a medium-sized geared turbofan engine mounted within a channel wing.

After close consideration of each design, it was apparent that Configuration 1 was too conventional to be considered an N+2 design. Configuration 4, on the other hand, was too advanced to be considered within an N+2 timeframe. A large scale wind tunnel test, being conducted by a competing NRA utilized a test model that was similar to Configuration 3 in that it was a blended wing body with circulation control[18]. Configuration 2 was considered to be at the appropriate level for the N+2 time frame. Further investigations into this design also showed that a 10' span model based on Configuration 2 would not exceed the load limits of all our perspective test locations. After consulting all involved in this project, it was decided that Configuration 2—the Hybrid blended-

Figure 3. Configuration 3 is a complete blended wing body with embedded engines.

Figure 4. Configuration 4 utilizes a high aspect ratio wing, in a diamond wing configuration.

Wing-Body—was best suited for the AMELIA test. Figure 5 shows a rendering of Configuration 2 in flight after

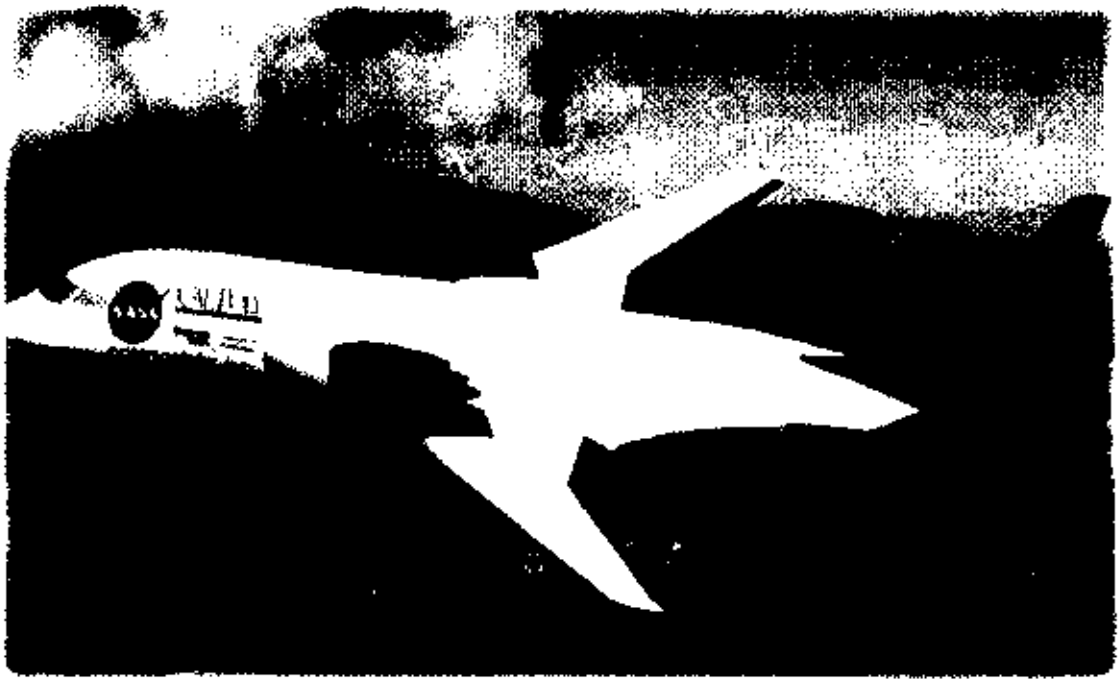

Figure 5. The final design iteration of Configuration 2; AMELIA's full scale conceptual model in flight above Hawaii.

many design refinement iterations.

B. AMELIA Design Features

In order to utilize the Configuration 2 geometry in a large-scale wind tunnel test setting, many design modifications were needed. The most significant alteration to the geometry came in the mounting system of the wind tunnel model. A sting was chosen as the ideal method to measure aerodynamic forces and moments, mainly for its ability to take measurements non-intrusively. Direct mounting of the model to the sting through the aft end raised concerns with disturbing the flow around the beaver tail. An underbody mount was designed to provide an attachment location with minimal flow disturbance. The mount is faired with a clamshell blade that extends vertically from the sting tip. The blade mount also serves to extend the negative angle of attach limit. Figure 6 shows a three view drawing of the model mounted to the blade attachment with empennage removed and relevant dimensions shown. The tail empennage is not shown in the three-view because it will not be attached to the model during the majority of the testing, due to the fact that the main focus of the testing is on aeroacoustic and aerodynamic measurements of the power lift system. The strakes, structural rudder and V-tail as seen in Fig. 5 were manufactured in order to supplement subsequent research and testing. These surfaces attach to the model via off blocks.

The selected configuration utilizes an optimized supercritical airfoil[19,20] with a dual radius flap at the trailing edge[21]. In order to minimize cost and complexity of the model, dual radius flaps of 0°, 30°, 60° and 90° deflections were proposed to be manufactured, as opposed to a mechanical flap where the deflection angle can be varied. The 90° flap deflection was later changed to 80° due to issues with the manufacturing of the flap with the appropriate blowing slot height. The flaps of the Configuration 2 design were also modified to be a single continuous flap for each wing, in order to reduce the amount of flow disturbance from discontinuities of the flap surface as well as allowing for less complicated configuration changes while the model is mounted on the sting. A cut away view of the model, with the 0° and 80° flap, is shown in Fig. 7. Figure 7 also highlights many of AMELIA's unique features, such as the internal flow control systems, the balance block, and the support structure for the over the wing mounted engines.

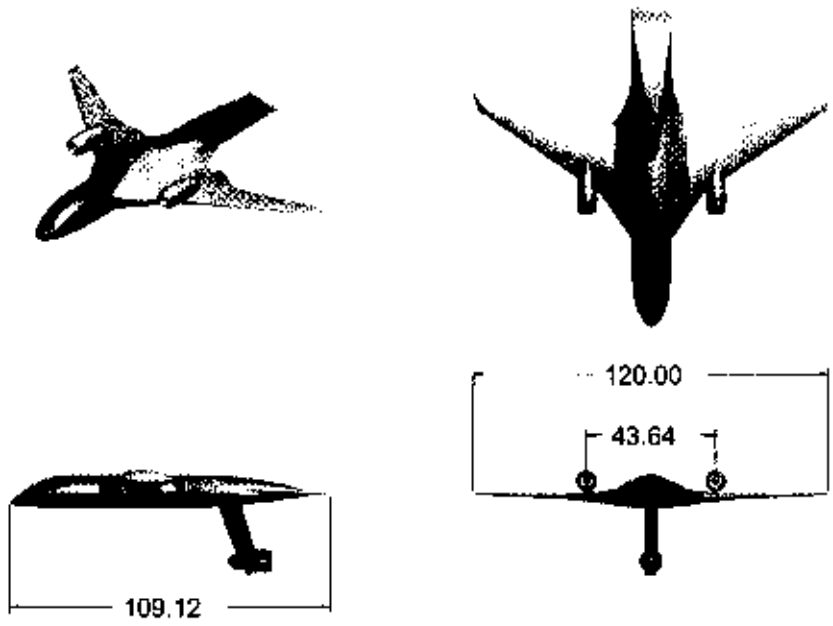

*Note: All Dimensions In Inches

Figure 6. A three-view drawing of AMELIA with sting-blade attachment and tail surfaces removed.

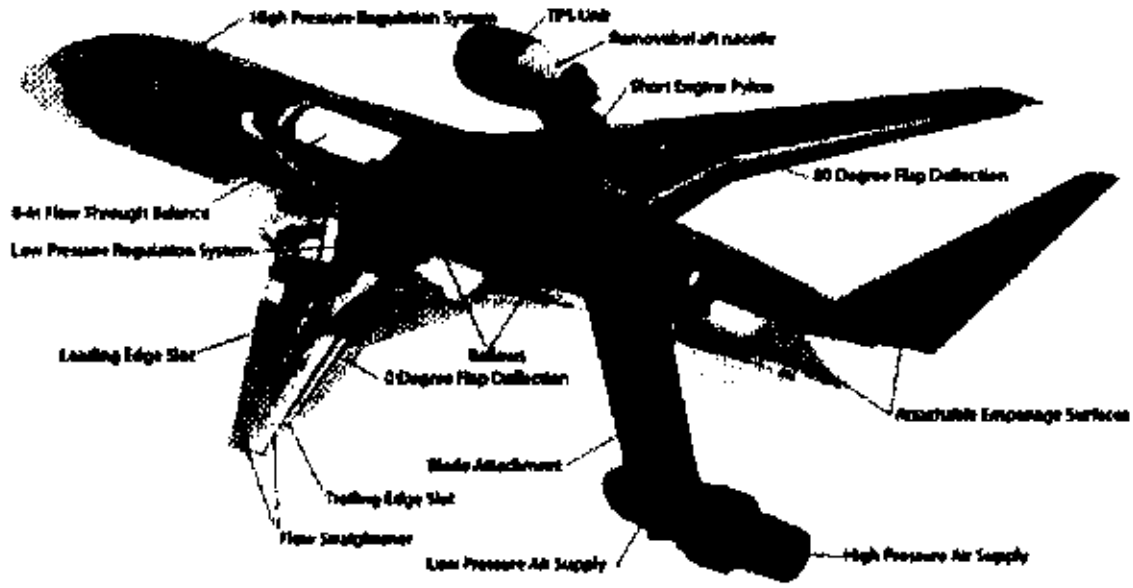

Figure 7. A section view of AMELIA, revealing the complex internal components highlighting the flow system for the powered lift system and the flow-though balance.

C. High and Low Pressure Air Systems

Plumbing for preassureized-heated air enters the model though the sting-blade attachment supplying the necessary high and lower pressure air for the powered lift system. The larger blue fixture shown at the bottom of the

schematic in Fig. 7 is the entry point for the high-pressure air required to power the Turbine Propulsion Simulator (TPS) units. This system (600 psi maximum determined by the limits of the flow through balance provided by the Triumph Group) first travels through the NFAC provided sting into the fabricated sting-blade attachment making two approximately 90o turns before entering the 8" flow though balance. On the downstream side of the balance a separate flow control plenum and system regulates the air flow to the left and right TPS units. The airflow is adjusted using conical plugs that can be remotely controlled while the tunnel is in operation. The conical plugs are driven using MMP 24vdc gearmotors, and use linear potentiometers for position feedback. The plugs can be positioned to provide from 0-100% mass flow. The TPS unit flow is supplied through stainless steel pipes that attach to wing mounted pylons. Figure 8a shows the complete piping and mass flow control plenum for the high pressure air system along with the sting-blade attachment while 8b is a head on view of the downstream flow control system highlighting the staggered plumping layout necessary to rout the pressurized line to each of the TPS units.

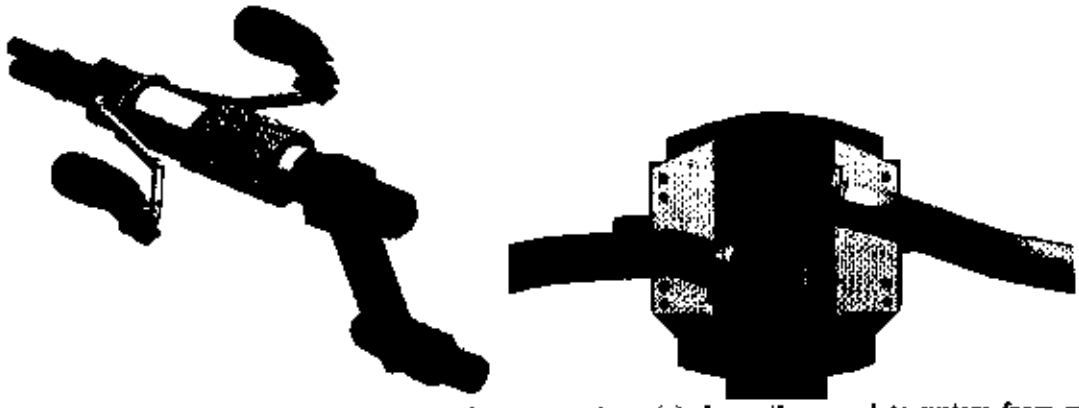

Figure 8. A schematic of the high pressure air system where (a) shows the complete system from model entry to the TPS units and (b) shows a head on view of the downstream mass flow control system.

The low pressure system (approximately 100 psi) will be used to supply the air to the plenums that feed the slots at the leading and trialing edges for the circulation control wing. This system is fed via a pipe attached to the underside of the sting arm, which connects to the blade body. Air travels up the blade where it is split into the left and right wings allowing for the conversion of non-metric to metric to be made though a two bellows system. Once the flow becomes metric on each wing the air is dispersed into low pressure plenum, shown purple in Fig. 9a and 9b. Each low pressure plenum consists of four butterfly valves controlled via 24vdc gear motors, with rotary pots for feedback allowing each of the slot plenums separate flow control from 0-100%. The flow to each slot plenums will be remotely controlled allowing for quick response time during tunnel operation.

Figure 9. A schematic of the low pressure air system where (a) shows the complete system for the left wing including the plenums and plumping thought be sting blade attachment and (b) shows the structure for the internal mass flow control system for each of the four slot plenums in the left wing.

D. Turbine Propulsion Simulators

The turbine propulsion simulators were incorporated in the wind tunnel model as an attempt to replicate the exhaust flow of a turbofan engine. One of the primary research objects in this investigation is the ability to entrain engine exhaust from upper surface blowing with the flow from the circulation control wing. As a means to evaluate this entrainment ability, two separate engine heights will be investigated during testing. Height adjustments will be completed using faired structural pylons.[22,23] These pylons also act as pressure vessels within which the high pressure air is fed to the TPS units. Altering the model for engine height adjustments is projected to be the most time consuming modification and therefore will be kept to a minimum to decrease time in the tunnel.

The turbine propulsion simulators are TDI model 441 simulators on loan from NASA Langley. Internal to the 441, compressed air powers a three stage turbine, which drives the two stage fan. The units are capable of producing 175 lbs of thrust, at 6.5 lb/s total mass flow rate. The TPS units are heavily instrumented with thermocouples, total probes, and static ports, an accelerometer, and a RPM pick-up in order to permit thorough health monitoring during testing. In the case of a TPS unit failure, one back-up TPS unit has also been reconditioned and will be fitted with a nacelle and instrumentation. Additionally, the TPS will never be operated at its maximum operating condition; it is projected that the running the units at a derated value (approximately 80%) will extend the life of each unit.

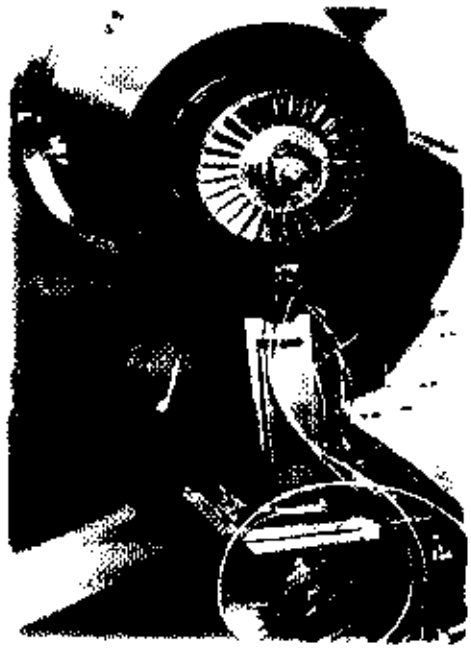

Figure 10. A photograph of the Model 441 TPS unit installed in the nacelle mounted on AMELIA.

Cal Poly has obtained the rights to barrow a controller from NASA Ames compatible with the 441 TPS units. The controller is LabVIEW based and will be capable of operating two TPS units simultaneously. The controller should be functional be early 2011. A basic overview of the controller wiring is given here: the simulator bearing thermocouple leads, rpm leads, and accelerometer leads for the two simulators is connected to an analog input card through to the front of the console. A oil flow signal and an oil flow control line from a separate lubrication cart is connected to the console. The console provides two output leads that can be used to trigger shutdown of an external air supply system if health limits are exceeded. During nominal operation, dedicated personal will set the air supply pressure as a function of rpm and will remain in the loop while the TPS is in operation as the safety officer.

E. Circulation Control Plenums

Circulation control flow is delivered to the upper surface of the wing via eight separate plenums at the leading and trailing edges. Supplied by the low pressure system, each plenum has one small entrance which creates an uneven pressure distribution and vorticular flow. In order to reduce this complex flow, a thin partition of aluminum foam is used as a flow straightener and a means to achieve constant back pressure along the length of the plenum. Downstream of the aluminum foam is a converging nozzle. The throat of the nozzle varies in size (proportionally with the plenum) along the spanwise direction. Each slot plenum is instrumented with three pitot probes to measure the internal pressure to insure the plenum is at constant pressure during operation. Figure 11 shows a cross section of the leading and trailing edge plenums with the metal foam placement for scale.

In the past circulation control experiments have had issues with accurately predicting the flow has been precise knowledge of the slot height under pressure. The height of the circulation control slot is an important factor in the calculation of momentum coefficient, which is used widely in circulation control analysis. Values for slot height are typically known to sufficient fidelity post manufacturing, however under pressure slot height can vary by a large factor. Successful application of a capacitance based slot height measurement device at NASA Glenn, lead us to believe that this technique may work well for the AMELIA model as well. The device is called the Capacitec GAPMAN, and utilizes a flexible wand, which can be taped to the lower surface of the slot/upper surface of the flap so that measurements can be made during testing. The calibration will include a thorough investigation of the use of

aluminum foam to provide flow straightening and uniform pressure. Each plenum will be calibrated and pressurized separately. With the model arriving at Cal Poly in the next month, one of the top priorities will be calibration of the slot flow.

Figure 11. A schematic showing the cross section of (a) the leading and (b) the trailing edge plenums highlighting the meat foam flow straighter placement.

F. Flow-Through Balance

The MC-130-8.00-Ai air balance will be utilized for the large scale wind tunnel test. The balance is being provided and calibrated by the Triumph Group. This particular balance is capable of operating with two separate flow systems at a maximum of 13 lb/s at 600 psi. AMELIA will be utilizing only one flow system for the high pressure portion of the powered lift system. Table 1 details the original maximum allowable loads for the MC-130-8.00-Ai air balance, where all expected loads for AMELIA are within the allowable limits.

Table 1. Original specifications for the MC-130-8.00-Ai air balance rated capacities (measured at the center of the balance)

Normal Force (NF)	Pitching Moment (PM)	Side Force (SF)	Yawing Moment (YM)	Rolling Moment (RM)	Axial Force (AF)
Lbs	in-lbs	Lbs	in-lbs	in-lbs	Lbs
13,000	107,250	3,000	18,000	32,000	500

III. AMELIA Instrumentation

The purpose of AMELIA is to provide both aeroacoustic and aerodynamic measurements to be used for current and future modeling validation efforts. Therefore it's imperative that the model be highly instrumented in order to capture the maximum amount of flow physics possible for our given budget and timeline. Almost all instrumentation placement occurs on the left wing and was chosen based on preliminary CFD results. Figure 12 is a half-span schematic of the model illustrating the relative placement of the static pressure ports and unsteady pressure transducers. The model is instrumented with 230 static pressure ports in five chordwise groups and one spanwise group (highlighted in red in Fig. 12). The five chodewise locations were chose in order to investigate flow over the wing starting from the most inboard sections as follows: Buttline (BL) 118 captures the interactions between the fuselage and wing, BL 240 investigates the flow downstream of the engine exit plane, BL 500 should capture the flow over the wing with the least amount of inboard or outboard effects, and BL 638 and 642 are positioned close to one another for a direct comparison of pressure distribution on the outboard section of the wing with and without circulation control. The 8 unsteady pressure transducers were placed such that the cabin noise and the wing interaction downstream of the engine exit plane can be studied.

Five static pressure ports are located on the right wing in order to verify symmetry in the pressure distribution. The right half of the model was intentionally left as uninstrumented as possible to allow for global skin friction measurements using FISF, for more information about this technique for AMELIA please refer to Part 2: Preparation for Wind Tunnel Model Testing and Verification of Cal Poly's AMELIA 10 Foot Span Hybrid Wing-Body Low Noise CESTOL Aircraft).

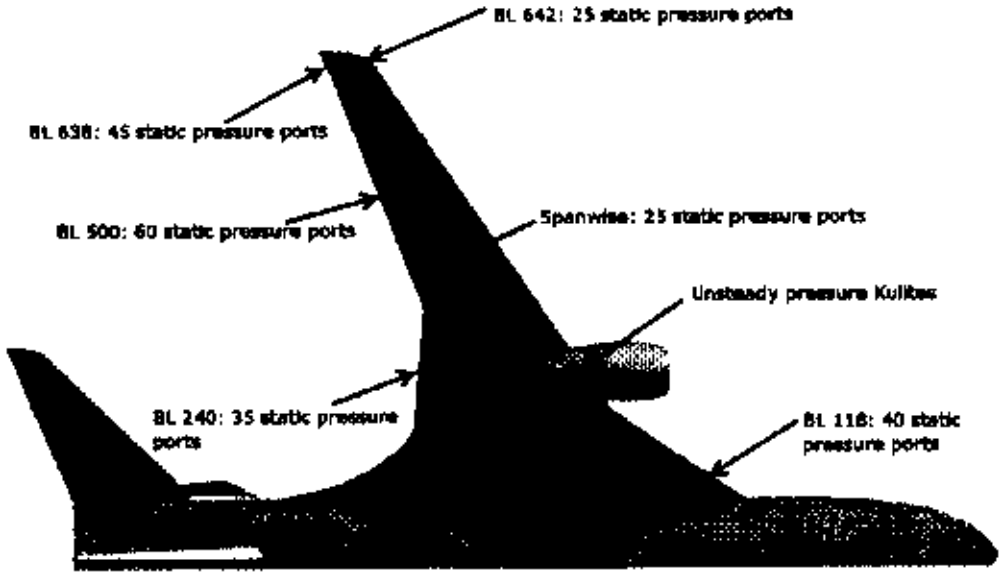

Figure 12. A schematic showing all external locations of the static pressure ports and the unsteady pressure transducers.

IV. AMELIA Fabrication

Patersonlabs, Inc. competed and won the contact to manufacture the 10 ft span model. Fabrication of the model stated in the second year of the project and it is projected that the model will be completed by the end of January of 2011. Currently Patersonlabs, Inc. has completed machining all elements of the model, including all outer mold lines, the high and low pressure air system, all internal plumbing had been routed, all static pressure taps and unsteady pressure ports have been installed, all flaps have been instrumented, and with the nacelles for the TPS. Figure 13 shows photographs of AMELIA before and after the paint without the nacelles installed. Figure 14 shows the low and high pressure air control systems, respectively. Currently, AMELIA is undergoing hydrostatic proof testing, awaiting completion it will receive one more coat of paint, and the final stress analysis will be delivered to Cal Poly also by the end of January. Cal Poly has been receiving regular progress reports from Patersonlabs, Inc and is in constant communication regarding manufacturing process and needs.

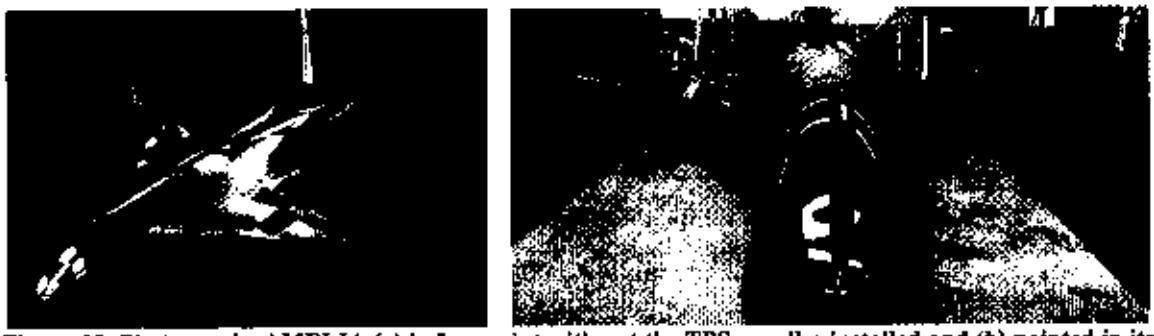

Figure 13. Photographs AMELIA (a) before paint with out the TPS nacelles installed and (b) painted in its final configuration without the TPS nacelles installed.

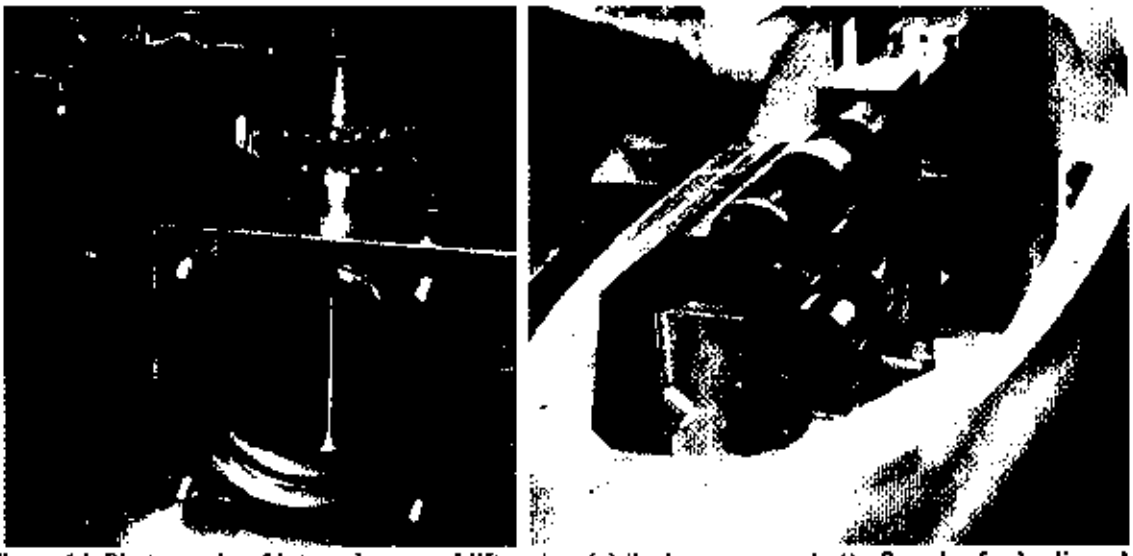

Figure 14. Photographs of internal powered lift system (a) the low pressure butterfly valve for leading edge slot plenum control and (b) the high pressure mass flow control system for the left and right TPS units.

Acknoldgements

This work was funded as part of a NASA Research Announcement award under Contract #NNL07AA55C with Craig Hange and Clif Horne as the technical monitors. The authors wish to thank all of the students who have participated in this work so far; their hard work and dedication have been invaluable to this research.

References

[1]Collier F. Overview of NASA's environmentally responsible aviation (ERA) project. 2009 Fundamental Aeronautics Conference, Atlanta GA, oral presentation, 2009.

[2]Madugundi D, Nagib H and Kiedaisch J. Evaluation of turbulence models through prediction of separated flows with and without flow control and circulation effects. *46th AIAA Aerospace Sciences Meeting and Exhibit*, AIAA, Reno NV, AIAA-2008-0567, 2008.

[3]McGowan G and Gopalarathnam A. Computational study of circulation control airfoil using FLUENT. *Applications of Circulation Control Technology*, edited by R. D. Joslin and G. S. Jones, Vol. 214 of Progress in Astronautics and Aeronautics, chap. 21, American Institute of Aeronautics and Astronautics, Inc., pp. 539-554, 2006.

[4]McGowan G, Gopalarathnam A, Xiao X, and Hassan H A. Role of turbulence modeling in flow prediction of circulation control airfoils. *Applications of Circulation Control Technology,* edited by R. D. Joslin and G. S. Jones, Vol. 214 of Progress in Astronautics and Aeronautics, chap. 19, American Institute of Aeronautics and Astronautics, Inc., pp. 499-510, 2006.

[5]Liu, Y., Sankar, L. N., Englar, R. J., Ahuja, K. K., and Gaeta, R. J. Computational evaluation of steady and pulsed set effects on a circulation control airfoil. *Applications of Circulation Control Technology*, edited by R. D. Joslin and G. S. Jones, Vol. 214 of Progress in Astronautics and Aeronautics, chap. 22, American Institute of Aeronautics and Astronautics, Inc., pp. 557-577, 2006.

[6]Chang III P A, Slomski J, Marino,T, Ebert M P, and Abramson J. Full Reynolds-stress modeling of circulation control airfoil. *Applications of Circulation Control Technology*, edited by R. D. Joslin and G. S. Jones, Vol. 214 of Progress in Astronautics and Aeronautics, chap. 17, American Institute of Aeronautics and Astronautics, Inc., pp. 445-466, 2006.

[7]Paterson E G and Baker W J. RANS and detached-eddy simulation of the NCCR airfoil. *Applications of Circulation Control Technology*, edited by R. D. Joslin and G. S. Jones, Vol. 214 of Progress in Astronautics and Aeronautics, chap. 16, American Institute of Aeronautics and Astronautics, Inc., pp. 421-444, 2006.

[8]Baker W J and Paterson E G. Simulation of steady circulation control for the general aviation circulation control (GACC) Wing. *Applications of Circulation Control Technology*, edited by R. D. Joslin and G. S. Jones, Vol. 214 of Progress in Astronautics and Aeronautics, chap. 20, American Institute of Aeronautics and Astronautics, Inc., pp. 513-537, 2006.

[9]Sahu J. Time-accurate simulations of synthetic jet-based flow control for a spinning projectile. *Applications of Circulation Control Technology*, edited by R. D. Joslin and G. S. Jones, Vol. 214 of Progress in Astronautics and Aeronautics, chap. 23, American Institute of Aeronautics and Astronautics, Inc., pp. 579-596, 2006.

[10]Zha G C and Paxton C D. Novel flow control method for airfoil performance enhancement using co-flow jet. *Applications of Circulation Control Technology*, edited by R. D. Joslin and G. S. Jones, Vol. 214 of Progress in Astronautics and Aeronautics, chap. 10, American Institute of Aeronautics and Astronautics, Inc., pp. 293-314, 2006.

[11]McGowan G, Rumsey C. L, Swanson R C, and Hassan H A. A three-dimensional computational study of a circulation control wing. *3rd AIAA Flow Control Conference*, AIAA, San Francisco CA, AIAA-2006-3677, 2006.

[12]Owen F K. Measurement and analysis of circulation control airfoils. *Applications of Circulation Control Technology*, edited by R. D. Joslin and G. S. Jones, Vol. 214 of Progress in Astronautics and Aeronautics, chap. 4, American Institute of Aeronautics and Astronautics, Inc., pp. 105-112, 2006.

[13]Cerchie D, Halfon E, Hammerich A, Han G, Taubert L, Trouve L, Varghese P, and Wygnanshi I. Some circulation and separation control experiments. *Applications of Circulation Control Technology*, edited by R. D. Joslin and G. S. Jones, Vol. 214 of Progress in Astronautics and Aeronautics, chap. 5, American Institute of Aeronautics and Astronautics, Inc., pp. 113-166, 2006.

[14]Munro S E, Ahuja K K, and Englar R J. Noise reduction through circulation control. *Applications of Circulation Control Technology*, edited by R. D. Joslin and G. S. Jones, Vol. 214 of Progress in Astronautics and Aeronautics, chap. 6, American Institute of Aeronautics and Astronautics, Inc., pp. 167-190, 2006.

[15]Jones G S. Pneumatic Flap Performance for a two-dimensional circulation control airfoil. *Applications of Circulation Control Technology*, edited by R. D. Joslin and G. S. Jones, Vol. 214 of Progress in Astronautics and Aeronautics, chap. 7, American Institute of Aeronautics and Astronautics, Inc., pp. 191-244, 2006.

[16]Englar R J. Experimental Development and evaluation of pneumatic powered-lift super-STOL aircraft. *Applications of Circulation Control Technology*, edited by R. D. Joslin and G. S. Jones, Vol. 214 of Progress in Astronautics and Aeronautics, chap. 7, American Institute of Aeronautics and Astronautics, Inc., pp. 191-244, 2006.

[17]Warwick G. Boeing works with airlines on commercial blended wing body freighter. Flight International, 2007.

[18]Collier F, Zavala E, and Huff D. Fundamental aeronautics program, subsonic fixed wing reference guide. NASA.

[19]Marshall, D., and Jameson, K., "Overview of Recent Circulation Control Modeling Activities at Cal Poly", AIAA-2010-348, AIAA 48th Aerospace Sciences Meeting and Exhibit, Orlando, Fla.

[20]Lane K A and Marshall D D. A surface parameterization method for airfoil optimization and high lift 2D geometries utilizing the CST methodology. *47th AIAA Aerospace Sciences Meeting and Exhibit*, AIAA, Orlando FL, AIAA-2009-1461, 2009.

[21]Lane K A and Marshall D D. Inverse airfoil design utilizing CST parameterization. *48th AIAA Aerospace Sciences Meeting and Exhibit*, AIAA, Orlando FL, AIAA-2010-1228, 2010.

[22]Golden R and Marshall D D. Design and performance of circulation control flap systems," *48th AIAA Aerospace Sciences Meeting and Exhibit*, AIAA, Orlando FL, AIAA 2010-1053, 2010.

[23]Englar R J, Gaeta R J, Lee W J and Leone V. Development of pneumatic over-the-wing powered-lift technology; part I: aerodynamic propulsive. *27th AIAA Applied Aerodynamics Conference*, AIAA, San Antonio TX, AIAA-2009-3942, 2009.

[24]Gaeta R J, Englar R J and Avera M. Development of pneumatic over-the-wing powered lift technology art II: aeroacoustics. *27th AIAA Applied Aerodynamics Conference*, AIAA, San Antonio TX, AIAA-2009-3941, 2009.